Electronic spectra of sulfur difluoride radicals between 295 and 495 nm observed with resonance-enhanced multiphoton ionization spectroscopy

2 AUTHORS:

Russell Johnson
National Institute of Standards and Technology
77 PUBLICATIONS **1,272** CITATIONS

SEE PROFILE

Jeffrey W Hudgens
National Institute of Standards and Technology
135 PUBLICATIONS **2,251** CITATIONS

SEE PROFILE

Electronic Spectra of SF$_2$ Radicals between 295 and 495 nm Observed with Resonance-Enhanced Multiphoton Ionization Spectroscopy

Russell D. Johnson III and Jeffrey W. Hudgens*

Chemical Kinetics Division, National Institute of Standards and Technology,[†] Gaithersburg, Maryland 20899
(Received: September 29, 1989)

Spectra of the SF$_2$ radical were observed between 295 and 495 nm by 2 + 1, 2 + 2, and 3 + 1 resonance-enhanced multiphoton ionization (REMPI) spectroscopy. Vibrational progressions associated with two Rydberg states were assigned. The $\tilde{B}$ $^1B_1$ (4s) Rydberg state was characterized with the spectroscopic values $\omega'_1(a_1$ sym str$) = 991$ (12) cm^{-1}, $\omega'_2(a_1$ bend$) = 361$ (24) cm^{-1}, and $T_0 = 54433$ cm^{-1}. The $\tilde{E}$ (4p) Rydberg state was characterized by the values $\omega'_1(a_1$ sym str$) = 931$ (59) cm^{-1}, $\omega'_2(a_1$ bend$) = 383$ (42) cm^{-1}, and $T_0 = 62015$ cm^{-1}. Evidence for the $\tilde{C}$ state which lies between 57 000 and 60 000 cm^{-1} is presented. The SF$_2$ was produced by a variety of methods, including passing SF$_6$ through a microwave discharge, which provides direct evidence that discharges produce SF$_2$ radicals.

Introduction

Sulfur fluoride radicals are believed to play major reactive roles in commercially important plasma processes. The semiconductor industry uses plasmas to etch circuit features into silicon wafers. Reactive plasmas formed from SF$_6$/O$_2$ mixtures produce particularly rapid etch rates.[1] The electric power industry uses SF$_6$ gas as a dielectric insulator in high-voltage circuit breakers and other devices. Plasmas created by corona discharges within these devices generate undesirable, highly toxic gases including S$_2$F$_{10}$.[2,3,22] If accurate reaction models of these commercial processes were constructed from basic chemical kinetic data, such models might discover ways to improve these commercial processes. However, the present chemical kinetic data[4] for SF$_x$ (x = 1, 2, 3, 5) radicals are too meager. Even the optical methods needed to sensitively detect SF$_x$ (x = 2, 3, 5) sulfur fluoride radicals in kinetic studies do not exist.

This paper reports new spectroscopy of the SF$_2$ radical observed by resonance-enhanced multiphoton ionization (REMPI) spectroscopy. We have detected three new electronic states using 2 + 1, 2 + 2, and 3 + 1 REMPI excitation schemes. We present a thorough analysis of two of these states. These REMPI bands enable the sensitive detection of SF$_2$ radicals in diverse reactive environments.

Modern spectroscopic methods have played a significant historical role in the study of SF$_2$ chemistry. On the basis of the prediction that SF$_2$ has particularly strong sulfur fluorine bonds, early workers believed that SF$_2$ would be very stable. Several groups had reported its synthesis.[5] However, in 1969 microwave spectroscopy[6] and mass spectrometry[7] showed that SF$_2$ is a chemically unstable transient. The microwave spectroscopic data showed that SF$_2$ possesses a C_{2v} structure with a F-S-F bond angle of 98.2°.[6,8,9] Subsequent studies in the gas phase[8–10] and in matrices[11,12] have measured the three SF$_2$ vibrational frequencies.

The ground state electronic configuration of the SF$_2$ radical is

$$...5a_1^2 3b_2^2 6a_1^2 2b_1^2 7a_1^2 4b_2^2 1a_2^2 5b_2^2 8a_1^2 3b_1^2 \qquad \tilde{X} \ ^1A_1$$
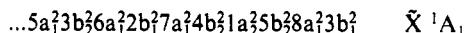
De Leeuw et al.[13] have observed the photoelectron spectrum of SF$_2$ and measured the ionization potentials of the highest six occupied orbitals. They found that the formation of the $\tilde{X}$ $^2B_1$ SF$_2$ cation required 10.08 eV.

Until recently, no excited electronic states of SF$_2$ radicals were known. Glinski[14] has identified SF$_2$ radical as the carrier of an emission spectrum that extends between 550 nm and the infrared region. This emission probably arises from the lowest lying valence state ($T_0 \sim 18\,200$ cm^{-1}) formed by the promotion of an electron from the HOMO 2b$_1$ orbital to the LUMO 5a$_1$ orbital. This state should possess the configuration

$$...5b_2^2 8a_1^2 3b_1^2 9a_1 \qquad \tilde{A} \ ^1B_1$$
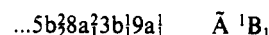
Much uncertainty surrounds the kinetic properties of the SF$_2$ radical. Among these uncertainties is whether gas mixtures of SF$_6$ passed through a microwave discharge contain SF$_2$ radicals. De Leeuw et al.[13] attempted to generate SF$_2$ radicals with a microwave discharge of SF$_6$ but did not detect a SF$_2$ photoelectron spectrum. However, on the basis of the chemistry observed from flows of microwave discharged SF$_6$, it has been proposed that SF$_2$ is produced.[15] A study that used plasma etching by SF$_6$/O$_2$ mixtures also suggests that SF$_2$ is an important product.[16] Our present REMPI study resolves this question by directly observing SF$_2$ radicals within the effluent from a microwave discharge of SF$_6$.

Methods and Apparatus

The apparatus and procedures are fully described elsewhere.[17] Briefly, SF$_2$ radicals were produced in a flow reactor operated at ~2 Torr by methods described below. A portion of the flow reactor effluent that contained SF$_2$ radicals effused into a high-vacuum chamber (~5 × 10^{-5} Torr) and was ionized by a focused laser beam. The ions were extracted into a time-of-flight mass spectrometer, detected with a gated integrator, and averaged and archived by a computer data acquisition system. The spectrum presented here consists of the mass-selected m/z 70 ion current

(1) d'Agostino, R.; Flamm, D. L. *J. Appl. Phys.* **1981**, *52*, 162.
(2) Janssenn, F. J. J. G. *Kema Sci. Tech. Rep.* **1984**, *2*, 9.
(3) Griffin, G. D.; Easterly, C. E.; Sauers, I.; Ellis, H. W.; Christophorou, L. G. *Tox. Environ. Chem.* **1984**, *9*, 139.
(4) Herron, J. *Int. J. Chem. Kinet.* **1987**, *19*, 129.
(5) A review of the history, synthesis, and chemistry of the lower sulfur fluorides is found in: Seel, F. *Adv. Inorg. Chem. Radiochem.* **1974**, *16*, 297.
(6) Johnson, D. R.; Powell, F. X. *Science* **1969**, *164*, 950.
(7) Seel, F.; Heinrich, E.; Gombler, W.; Budenz, R. *Chimia* **1969**, *23*, 73.
(8) Kirchhoff, W. H.; Johnson, D. R.; Powell, F. X. *J. Mol. Spectrosc.* **1973**, *48*, 157.
(9) Endo, Y.; Saito, S.; Hirota, E. *J. Mol. Spectrosc.* **1979**, *77*, 222.
(10) Deroche, J. C.; Burger, H.; Schulz, P.; Willner, H. *J. Mol. Spectrosc.* **1981**, *89*, 269.
(11) Haas, A.; Willner, H. *Spectrochim. Acta* **1978**, *34A*, 541.
(12) Willner, H. *Z. Anorg. Allg. Chem.* **1981**, *481*, 117.
(13) De Leeuw, D. M.; Mooyman, R.; De Lange, C. A. *Chem. Phys.* **1978**, *34*, 287.
(14) (a) Glinksi, R. *J. Chem. Phys. Lett.* **1986**, *129*, 342. (b) Glinski, R. J.; Mishalanie, E. A.; Birks, J. W. *J. Photochem.* **1987**, *37*, 217. The emission spectra reported in these papers were assigned to the FCS radical but are reassigned to the SF$_2$ radical in: (c) Glinksi, R. J. *Chem. Phys. Lett.* **1989**, *155*, 511.
(15) Plumb, I. C.; Ryan, K. R. *Plasma Chem. Plasma Proc.* **1986**, *6*, 247.
(16) Ryan, K. R.; Plumb, I. C. *Plasma Chem. Plasma Proc.* **1988**, *8*, 263.
(17) Johnson III, R. D.; Tsai, B. P.; Hudgens, J. W. *J. Chem. Phys.* **1988**, *89*, 4558.

*Address correspondence to this author.
†Formerly known as the National Bureau of Standards.

as a function of laser wavelength. The dye laser was calibrated by the optogalvanic method[18] using a table of neon lines.[19]
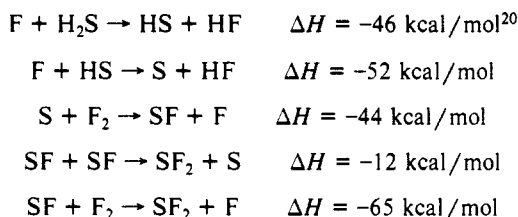
Two different dye lasers were used during these experiments. The output of a Nd:YAG pumped dye laser was doubled and focused with a 100-mm lens. The dyes, frequency-doubled spectral ranges, and output energies used to collect data were rhodamine 6G (283–288 nm, 7 mJ/pulse), kiton red (291–297 nm, 5 mJ/pulse), sulforhodamine 640 (302–308 nm, 2.5 mJ/pulse), and LDS 698 (308–326 nm, 2.5 mJ/pulse). The output of a XeCl excimer pumped dye laser was focused with a 250-mm lens. The dyes, spectral ranges, and output energies used were *p*-terphenyl (330–350 nm, 21 mJ/pulse), DMQ (350–370 nm, 18 mJ/pulse), and QUI (370–390 nm, 35 mJ/pulse). In addition, the following dyes were pumped with the XeCl excimer laser and focused with a 100-mm lens: coumarin 460 (440–460 nm, 32 mJ/pulse) coumarin 480 (460–495 nm, 31 mJ/pulse).

Results and Analysis

Identification of the Spectral Carrier. During this study of SF_2 radicals four different gas mixtures and two protocols were used to produce SF_2 in a flow reactor maintained at 1–2 Torr of total pressure. In one protocol gas mixtures were passed through a microwave discharge and then flowed 40 cm (at ~ 3 m/s) to a sampling orifice. The sampling orifice admitted a portion of the gas into the mass spectrometer ionization region. The unsampled gas mixture passed from the flow reactor into a vacuum pump. Two gas mixtures were used with this procedure: (1) a 1% concentration of SF_6 diluted in helium; (2) a mixture of 1% H_2S and 2% F_2 diluted in helium.

In a second protocol a 1% concentration of F_2 in helium was passed through the microwave discharge. The dilute mixture of helium and fluorine atoms flowed down a passivated tube toward the sampling orifice at 1–3 m/s. At 2–8 mm upstream from the sampling orifice either (3) H_2S or (4) CS_2 was added to the gas stream. Bimolecular reactions within the reaction zone produced the SF_2 radicals.

The reaction chain of the $F + H_2S$ reaction systems undoubtably included

$$F + H_2S \rightarrow HS + HF \quad \Delta H = -46 \text{ kcal/mol}^{20}$$

$$F + HS \rightarrow S + HF \quad \Delta H = -52 \text{ kcal/mol}$$

$$S + F_2 \rightarrow SF + F \quad \Delta H = -44 \text{ kcal/mol}$$

$$SF + SF \rightarrow SF_2 + S \quad \Delta H = -12 \text{ kcal/mol}$$

$$SF + F_2 \rightarrow SF_2 + F \quad \Delta H = -65 \text{ kcal/mol}$$

All production methods used during this study could have also generated higher SF_x ($x = 3$–6) species via the fluorine addition reactions

$$SF_y + F_2 \rightarrow SF_{y+1} + F$$

$$SF_y + F \rightarrow SF_{y+1}$$
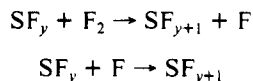
and to a lesser extent through disproportionation reactions

$$SF_x + SF_y \rightarrow SF_{x+1} + SF_{y-1}$$
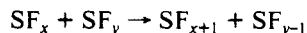
Radical generation methods 3 and 4 produced the strongest SF_2 REMPI signals. All SF_2 production methods produced identical optical spectra. The optical spectra were always carried by $^{32}SF_2^+$ (m/z 70). Whenever the microwave discharge was extinguished, the REMPI signals ceased. No ion signals appeared at masses corresponding to SF_x ($x = 3$–6) or to S_yF_x ($y = 2, 3, ...; x = 2, 3, 4, ...$) cations. The vibrational assignments conform to those
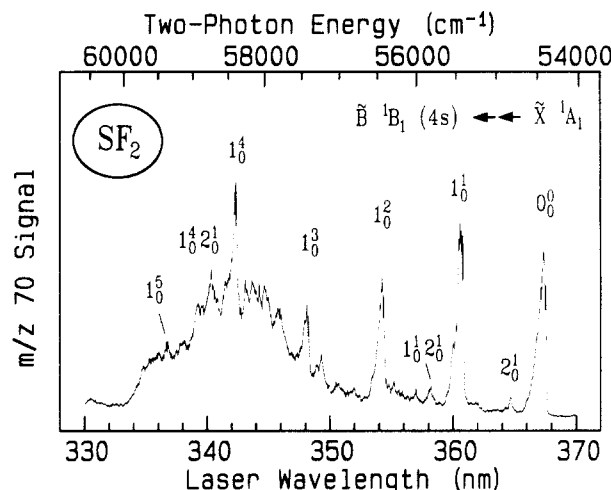

Two-Photon Energy (cm⁻¹)

Figure 1. Composite REMPI spectrum of the $^{32}SF_2$ radical (m/z 70) between 330 and 370 nm.

expected to the SF_2 radical. Thus, all chemical and spectroscopic evidence support the assignment of these REMPI spectra to the SF_2 radical.

The $\tilde{B}$ $^1B_1$ (4s) $\leftarrow\leftarrow$ $\tilde{X}$ $^1A_1$ Band System. Figure 1 shows the m/z 70 REMPI spectrum of SF_2 between 330 and 370 nm. Table I lists the observed band maxima, state energies, and assignments. (That the spectrum arises from two photon resonances is shown below.) The REMPI spectrum displays two regularly spaced progressions. Six REMPI bands comprise the more intense progression. The red-most band of this intense progression lies at 367.32 nm. Six REMPI bands also comprise the weaker progression. This weak progression terminates at 364.69 nm, e.g., 394 cm⁻¹ higher in energy than the terminus of the strong progression. Within the measurement uncertainty both progressions exhibit the same frequency intervals, e.g., intense $2h\nu = 991$ (12) cm⁻¹, weak $2h\nu = 980$ (18) cm⁻¹. This similarity suggests that both progressions arise from the same upper electronic state (labeled the $\tilde{B}$ state in Table I) and that both progressions have one vibrational mode in common. Accordingly, we assign the source of the more intense progression to a series of 1_0^n ($n = 0$, 1, 2, ...) fundamental bands associated with the $\tilde{B}$ state. We assign the source of the weaker progression to a series formed from the 2_0^1 band and $1_0^n 2_0^1$ ($n = 1, 2, ...$) combination bands. These assignments characterize the $\tilde{B}$ state with the spectroscopic values: $\omega'_1(a_1 \text{ sym str}) = 991$ (12) cm⁻¹, $\omega'_2(a_1 \text{ bend}) = 361$ (24) cm⁻¹, and $T_0 = 54433$ cm⁻¹.

Between 330 and 369 nm SF_2 must absorb three photons to ionize and form the $\tilde{X}$ $^2B_1$ cation. The data indicate that the resonant state is prepared by the simultaneous absorption of two photons. Assuming two-photon preparation, the $\omega'_1(a_1 \text{ sym str})$ = 991 (12) cm⁻¹ of the $\tilde{B}$ state is similar to the vibrational frequency of the $\tilde{X}$ $^2B_1$ cation, $\omega_1 = 935$ (40) cm⁻¹. This similarity suggests that the $\tilde{B}$ state is a Rydberg state that possesses a $\tilde{X}$ $^2B_1$ cation core. The type of Rydberg orbital involved in this electronic state is determined by solving the Rydberg formula, $h\nu_{0-0}$ (cm⁻¹) = $IP_a - 109373/(n - \delta)^2$, for the adiabatic ionization potential, $IP_a = 81301$ cm⁻¹,[13] and the origin, $h\nu_{0-0} = 54433$ cm⁻¹. The only reasonable solution gives the principal quantum number of $n = 4$ and the quantum defect of $\delta = 1.98$. Quantum defects for ns, np, nd, and nf Rydberg states centered on sulfur should lie near $\delta \sim 2.0, 1.6, 0.08,$ and 0.06,[21] respectively. The solution for the $\tilde{B}$ state corresponds to the 4s Rydberg state. Thus, we

(18) King, D. S.; Schenck, P. K.; Smyth, K. C.; Travis, J. C. *Appl. Opt.* **1977,** *16,* 2617.

(19) Striganov, A. R.; Sventitskii, N. S. *Table of Spectral Lines of Neutral and Ionized Atoms*; Plenum: New York, 1968.

(20) Heats of formation were obtained from: Lias, S. G.; Bartmess, J. E.; Liebman, J. F.; Holmes, J. L.; Levin, R. D.; Mallard, G. *J. Phys. Chem. Ref. Data* **1988,** *17,* Suppl. 1.

(21) Manson, S. T. *Phys. Rev.* **1969,** *182,* 97.

(22) Van Brunt, R. J.; Olthoff, J. K.; Herron, J. T.; Savers, I. *Proc. 42nd Annu. Gaseous Electronics Conf., Bull. Am. Phys. Soc.,* in press.

(23) Van Brunt, R. J.; Siddagangappa, M. C. *Plasma Chem. Plasma Proc.* **1988,** *8,* 207.

(24) (a) Ryan, K. R. *Plasma Chem. Plasma Proc.* **1989,** *9,* 483. (b) Plumb, I. C.; Ryan, K. R. *Plasma Chem. Plasma Proc.* **1989,** *9,* 409.
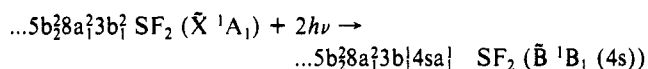
(25) Van Brunt, R. J.; Herron, J. T. *IEEE Trans. Electr. Insul.,* in press.

TABLE I: Band Maxima, Assignments, and Spacings Observed in the REMPI Spectrum of the $^{32}SF_2$ Radical between 330 and 490 nm[a]
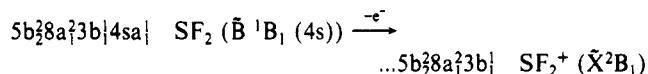
assign-ment	band max (λ_{air}), nm	state energy cm⁻¹	energy rel to $\tilde{B}$ ¹B₁ (4s) origin, cm⁻¹	energy rel to $\tilde{E}$ (4p) origin, cm⁻¹	ω_1' band interval, cm⁻¹	ω_2' band interval, cm⁻¹
			2-Photon Resonant States			
	372.67	53 651				
4s 2_1^0	369.84	54 063	−370			
4s 0_0^0	367.32	54 433	0			
4s 2_0^1	364.69	54 826	393			393
	361.87	55 253				
4s 1_0^1	360.68	55 435	1002		1002	
4s $1_0^1 2_0^1$	358.24	55 813	1380			378
	356.98	56 009				
	355.21	56 288				
4s 1_0^2	354.26	56 439	2006		1004	
4s $1_0^2 2_0^1$	351.99	56 804	2371			365
$\tilde{C}$	350.71	57 011				
$\tilde{C}$	349.31	57 239				
4s 1_0^3	348.14	57 432	2999		993	
4s $1_0^3 2_0^1$	345.94	57 797	3364			365
$\tilde{C}$	345.75	57 829				
$\tilde{C}$	344.69	58 007				
$\tilde{C}$	344.25	58 080				
$\tilde{C}$	343.66	58 180				
$\tilde{C}$	343.13	58 271				
$\tilde{C}$	342.38	58 397				
4s 1_0^4	342.28	58 415	3982		983	
$\tilde{C}$	341.48	58 552				
4s $1_0^4 2_0^1$	340.35	58 747	4314			332
$\tilde{C}$	339.24	58 938				
$\tilde{C}$	338.17	59 125				
$\tilde{C}$	336.79	59 367				
4s 1_0^5	336.66	59 390	4957		975	
$\tilde{C}$	336.04	59 499				
4s $1_0^5 2_0^1$	334.77	59 725	5292			335
			3-Photon Resonant States			
4p 0_0^0	483.62	62 015		0		
4p 2_0^1	480.51	62 416		401		401
4p 1_0^1	476.21	62 980		964	964	
4p 1_0^2	468.99	63 949		1934	970	
4p $1_0^2 2_0^1$	466.55	64 284		2269		335
4p 1_0^3	462.89	64 792		2777	843	
4p $1_0^3 2_0^1$	459.97	65 204		3189		412
4p 1_0^4	456.23	65 738		3723	946	

[a] The width of each REMPI band limits the measurement precision to ±0.25 nm (±30 cm⁻¹).

designate the $\tilde{B}$ state as $\tilde{B}$ ¹B₁ (4s). The spectral features arise from the two-photon excitation:

$$...5b_2^2 8a_1^2 3b_1^2 \; SF_2 \; (\tilde{X} \; {}^1A_1) + 2h\nu \rightarrow$$
$$...5b_2^2 8a_1^2 3b_1^1 4sa_1^1 \; SF_2 \; (\tilde{B} \; {}^1B_1 \; (4s))$$

SF₂ radicals in the $\tilde{B}$ ¹B₁ (4s) state may ionize through the process

$$5b_2^2 8a_1^2 3b_1^1 4sa_1^1 \; SF_2 \; (\tilde{B} \; {}^1B_1 \; (4s)) \xrightarrow{-e^-}$$
$$...5b_2^2 8a_1^2 3b_1^1 \; SF_2^+ \; (\tilde{X}^2 B_1)$$

Since this ionization step requires only 26 867 cm⁻¹, SF₂ ($\tilde{B}$ ¹B₁ (4s)) radicals can ionize after absorbing one laser photon. The overall ionization mechanism occurs through a 2 + 1 REMPI mechanism. The REMPI bands assigned to $\tilde{B}$ ¹B₁ (4s) ←← $\tilde{X}$ ¹A₁ transitions were carried only by SF₂⁺ (m/z 70). No evidence for photofragmentation of SF₂ cations was observed.

Further support for the assignment of the $\tilde{B}$ state to two-photon resonances is found by assigning the band at 369.84 nm as the 2_1^0 hot band. This hot band assignment gives ω''_2 (a₁ bend) = 370 (15) cm⁻¹ for the $\tilde{X}$ ¹A₁ state, which agrees with the value ω''_2 = 357 cm⁻¹, measured by gas-phase IR spectroscopy.

The 2_1^0 band is only 2% as intense as the 0_0^0 band. The weak intensity of this band was expected. All SF₂ radicals ionized by laser light of λ > 369 nm must absorb 4 photons rather than 3 to ionize. Thus, the 2_1^0 band is generated through a 2 + 2 process. The weakness of the 2_1^0 band may reflect—at least in part—the

lower ionization cross section of the 2 + 2 REMPI process as compared to a 2 + 1 REMPI process.

The $\tilde{C}$ ←← $\tilde{X}$ ¹A₁ Band System. A second REMPI band system carried by $^{32}SF_2^+$ (m/z 70) appears as an irregular series of closely spaced bands between 336 and 350 nm. In Table I this spectrum is assigned to an upper state labeled $\tilde{C}$. The band envelope of the m/z 70 REMPI signal shows two maxima that lie near 340 and 344 nm. Over part of the spectrum REMPI signals were also carried by $^{32}SF^+$ (m/z 51). The trace of this signal begins at 350 nm, steadily grows in intensity between 350 and 342 nm, reaches its maximum at 340 nm, and then follows the trace of the m/z 70 REMPI signal intensity associated with the $\tilde{C}$ ←← $\tilde{X}$ ¹A₁ band system. The m/z 51 REMPI trace does not emulate any feature associated with the $\tilde{B}$ ¹B₁ (4s) state, e.g., the 4s 1_0^4 band is absent from the SF⁺ (m/z 51) trace.

The data do not support a precise assignment of the electronic origin. We have assigned the $\tilde{C}$ state to reside at the energy of two photons (57 000–60 000 cm⁻¹). A lack of candidate states at other photon levels seems to assure this assignment. No candidate states reside at 1 photon of energy. States that lie at the 3-photon energy (e.g., Rydberg states that have excited cation cores) appear unreasonable. But four candidate states reside at the 2-photon energy level.

The leading candidate assignment for the $\tilde{C}$ state is the valence state that has the configuration and symmetry $...1a_2^2 5b_2^2 8a_1^2 3b_1^1 6b_2^1$ (¹A₂). In this configuration SF₂ can form the $\tilde{X}$ ²B₁ cation by absorbing only 1 photon, i.e., the m/z 70 signal would occur
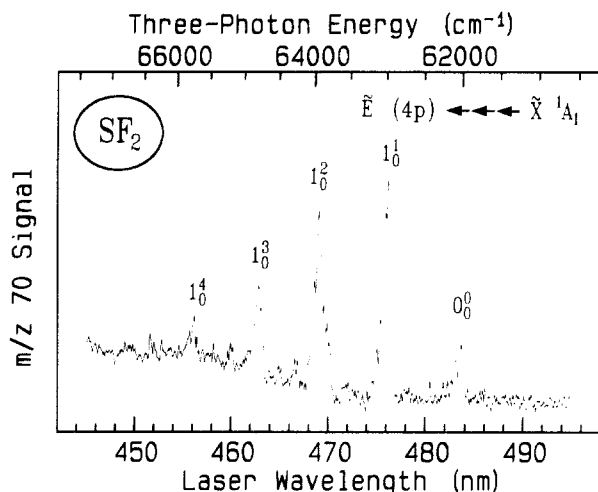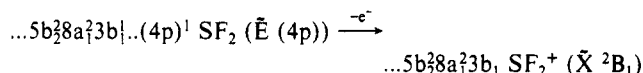
Figure 2. Composite 3 + 1 REMPI spectrum of the $^{32}SF_2$ radical (m/z 70) between 450 and 490 nm.

through a 2 + 1 REMPI mechanism. In this view subsequent photon absorption by SF_2^+ causes photofragmentation and generates the m/z 51 signal. Alternative assignments for the $\tilde{C}$ state possess the orbital configurations (and state symmetries) (a) $...1a_2^25b_2^28a_1^13b_1^29a_1$ ($^1A_1$), (b) $...1a_2^25b_2^28a_1^23b_1^29a_1$ ($^1B_2$), and (c) $...1a_2^25b_2^28a_1^23b_1^09a_1$ ($^1A_2$). Because SF_2 radicals in these configurations must form electronically excited cations, the ionization step requires 5.3–6.0 eV more energy than is needed to form $\tilde{X}$ $^2B_1$ cations. Signal generation through any of the alternate candidate states should occur through a 2 + 3 REMPI mechanism. Therefore, we doubt that a 2 + 3 REMPI mechanism can account for the moderate intensity displayed by the $\tilde{C}$ ←←← $\tilde{X}$ $^1A_1$ bands.

The $\tilde{E}$ (4p) ←←← *$\tilde{X}$ $^1A_1$ Band System.* Figure 2 shows the m/z 70 REMPI spectrum of SF_2 between 450 and 495 nm. In Table I we have labeled the electronic state that produces this spectrum as the $\tilde{E}$ state. Table I lists the band maxima observed between 450 and 495 nm, state energies, and assignments of the $\tilde{E}$ state. A similar, but extremely weak, REMPI spectrum was also observed between 300 and 325 nm. When we assume that the 300–325-nm spectrum (bands at 322.5 (0_0^0), 317.5 (1_0^1), 308.5 (1_0^3), 304.2 (1_0^4), and 302.5 ($1_0^42_0^1$) nm) arose from 2-photon resonances and that the 450–495-nm bands (Table I) arose from 3-photon resonances, the band energies of both spectra coincide. These coincidences show that the upper state lies between 62 000 and 66 000 cm^{-1}.

In Figure 2 the REMPI spectrum displays a moderately intense progression comprised of five bands and a weak progression comprised of three bands. An analysis similar to the one described above gives the spectroscopic values $\omega'_1(a_1$ sym str) = 931 (59) cm^{-1}, $\omega'_2(a_1$ bend) = 383 (42) cm^{-1}, and T_0 = 62015 cm^{-1}. The origin band lies at 483.62 nm. The close correspondence of ω'_1

frequencies between the $\tilde{E}$ state and the cation support an assignment of the $\tilde{E}$ state as a Rydberg state. Solving the Rydberg equation for the $\tilde{E}$ state origin gives the principal quantum number $n = 4$ and the quantum defect $\delta = 1.61$. This solution indicates that the $\tilde{E}$ state is a 4p Rydberg state. The 4p Rydberg orbitals are of symmetry a_1 ($4p_z$), b_1 ($4p_x$), and b_2 ($4p_y$), which give rise to state symmetries of $^1B_1$, $^1A_1$, and $^1A_2$. The spectra do not reveal the symmetry of the upper state. SF_2 radicals in the $\tilde{E}$ (4p) state may ionize through the process

$$...5b_2^28a_1^23b_1^1..(4p)^1\ SF_2\ (\tilde{E}\ (4p)) \xrightarrow{-e^-}$$

$$...5b_2^28a_1^23b_1\ SF_2^+\ (\tilde{X}\ ^2B_1)$$

Since this ionization step requires only $\sim$19 300 cm^{-1}, SF_2 ($\tilde{E}$ (4p)) radicals can ionize after absorbing 1 laser photon, i.e., the overall ionization mechanism occurs through a 3 + 1 REMPI mechanism. The REMPI bands assigned to $\tilde{E}$ (4p) ←←← $\tilde{X}$ $^1A_1$ transitions were carried only by SF_2^+ (m/z 70). No evidence for photofragmentation of SF_2 cations was observed.

Discussion

Spectroscopy of SF_2 Radicals. This study has identified two Rydberg states that contribute to the REMPI spectrum of the SF_2 radical. The vibrational assignments have established that the $\tilde{B}$ $^1B_1$ (4s) and $\tilde{E}$ Rydberg states reside at 54 433 and 62 015 cm^{-1}, respectively. The 2 + 1 and 3 + 1 REMPI spectra presented here enable the laser detection of these radicals. The $\tilde{B}$ $^1B_1$ (4s) ←←← $\tilde{X}$ $^1A_1$ 2 + 1 REMPI bands provide the better sensitivity.

Molecular orbital calculation of excited electronic states of the SF_2 radical could contribute much to the understanding of the spectra. Such calculations could determine the proper molecular orbital configuration of the $\tilde{C}$ state. Another curiosity of this study is the irregular intervals along the ω'_1 symmetric stretch in the $\tilde{E}$ (4p) Rydberg state. These variations seem too large to attribute to measurement uncertainty. The variation may reflect the presence of a valence perturbation or an undetected 4p Rydberg state of another symmetry.

Production of SF_2. The SF_2 production methods used during this study included microwave-sustained plasma. The spectroscopic detection of SF_2 radicals in the effluent from this plasma demonstrates that SF_2 is among the principal products. Because our experiment views the discharge effluent $\sim$130 ms after its production, our results do not show that SF_2 is a nascent discharge product. Our observations do show that the discharge effluent contains substantial quantities of SF_2 very shortly after production. Since the gas mixtures in commercial plasma reactors are relatively static, we conclude that SF_2 must be considered as an important constituent of the reactive medium. This observation is consistent with the stability of the SF_2 radical relative to other sulfur fluorides. Indeed, from our examination of just a few systems it appears that SF_2 is easily formed and will be often present in reactive systems involving sulfur and fluorine.